Polymer-Plastics Technology and Engineering, 53: 1598–1606, 2014

ISSN: 0360-2559 print/1525-6111 online
DOI: 10.1080/03602559.2014.919642

Improvement of Electron Transport Properties of Polypyrrole Nano-films by In-situ Polymerization under High Pressure

Jiansheng Wu[1,2], Dawei Gu[1], Jishu Li[1], Hongying Jiang[1], Qichun Zhang[2], and Linjiang Shen[1]

[1]*College of Science, Nanjing Tech University, Nanjing, China*
[2]*School of Materials Science and Engineering, Nanyang Technological University, Singapore*

The conducting polypyrrole (PPy) nanofilms have been in-situ polymerized on quartz substrates under various high reaction pressures (0.1–600 MPa). The effects of the applied pressure on films have been carefully investigated through UV-Vis, FT-IR, SEM, AFM and conductivity measurement. The effect of the applied pressure on the thickness and the electrical conductivity of the PPy films have been discussed. A three-dimensional relationship between film thickness, reaction pressure, and the conductivity of the films has also been described in text. Our results may provide a guide for studying in-situ polymerization of pyrrole and its derivatives under high reaction pressure.

Keywords Conductivity; High-pressure; Nanofilms; Polypyrroles; Processing

INTRODUCTION

Polypyrrole (PPy) has attracted a lot of attention in recent years since it offers a wide range of possible applications[1]. Normally, PPy can be prepared through in-situ polymerization in aqueous solution[2], and PPy films made by this method generally are highly charged and show high conductivity and high stability under ambient conditions[3–5]. Many applications based on PPy (e.g., transistors, sensor, actuator, supercapacitor and electrocatalysis[6–13]) have been widely demonstrated in the past few years. For most of these applications, the electronic conductivity is very important[14,15]. Several experiments have already showed that the conductivity of PPy thin film is strongly dependent on the polymerization temperature, mechanical stretching, or aging time[3,4,16–18]. However, polymerization under pressure, especially on very high pressure ($>10^8$ Pa), have a great effect on the conductivity and packing intensity as well as morphology. Our previous studies have already demonstrated that the reaction pressure greatly enhanced the performance of polyaniline (PANI) films[19–21]. Continuing on this research, we want to understand how the high reaction pressure affects the polymerization of pyrrole, the morphology of PPy films, and the physical properties of as-prepared films.

The present work focuses on the effect of reaction pressure on the in-situ polymerization and properties of PPy films. Under different reaction pressure (0.1–600 MPa), the conducting PPy films were successfully polymerized on quartz glass substrates. Both the characteristics of PPy films and the kinetic film growing were studied. The growth rate of PPy film was strongly related to the applied pressure in polymerization. Compared to the films polymerized under atmospheric pressure, high pressure-formed PPy films exhibit many novel characteristics including close packing, lower roughness and higher electrical conductivity. It is noteworthy that high pressure prepared PPy films have obvious differences in morphology, kinetics and conductivity compared to PANI films obtained at the same conditions.

EXPERIMENTAL

Materials

All chemicals used in this work were of analytical grade. Pyrrole was distilled in vacuum before use and other chemicals were directly used as received. Distilled water was used as a solvent in the case of all polymerization mixtures. Commercially available quartz glass slides (size in 6 mm × 10 mm, thickness in 1 mm) were used as substrates. Prior to use, all quartz glass substrates were cleaned by heating in a freshly prepared piranha solution at 70°C for 1 h, followed by extensive rinsing with distilled water. The piranha solution was made of 98% H_2SO_4 and 30% H_2O_2 in ratio of 7:3 by volume. Finally, the substrates were dried in vacuum at room temperature.

Preparation

PPy films were in-situ deposited on quartz substrate under pressures of 0.1, 100, 200, 300, 400, 500, and

Address correspondence to Prof. Linjiang Shen, College of Science, Nanjing Tech University, Nanjing, 210000, China. E-mail: ljshen@njtech.edu.cn or Prof. Qichun Zhang, School of Materials Science and Engineering, Nanyang Technological University, 50 Nanyang Avenue, 639798, Singapore. E-mail: qczhang@ntu.edu.sg

600 MPa, respectively. The oxidant/monomer ratio was chosen as 2.3 for preparing all samples. To prepare the reaction solution, 0.7 mL pyrrole in 25 mL DI water and 6.2 g $FeCl_3 \cdot 6H_2O$ in 25 mL DI water were mixed in an ice bath. After 10 sec, 3 mL of reaction solution was poured into a PTFE reaction vessel. The cleaned substrate covered with a thin adhesive tape on one side, was immersed into the reaction solution vertically. Polymerization time varied from 10 to 360 min, and polymerization temperature was kept constant at 5°C. During the reaction, the pressure was continually applied on the reaction vessel. After the reaction, the samples were washed by distilled water three times and dried in vacuum at room temperature.

Characterization

The thickness and surface morphology of PPy films were measured by Benyuan CSPM-5000 AFM in a contact mode. The SEM images were obtained on JEOL-JSM-5900 operating at an acceleration voltage of 15 kV. All samples were coated with a gold dispersion before the SEM study.

The absorption spectra were recorded on a UV–Vis spectrophotometer Analytik Jena Specord 50, with the wavelength ranging from 300 to 1100 nm and an uncoated quartz substrate as a reference. The optical properties of as-prepared samples were examined on a Harrick GATR accessory on a Bruker Vertex 70 FT-IR spectrometer. For comparison, a FT-IR spectrum for uncoated quartz substrate was also measured.

The electrical resistance R was measured by Keithley 2700 Digital Multimeter and Keithley 2400-C Source Meter with four-probe technique at room temperature. The four electrodes from Switzerland were made of RS electrically conductive paint. The distance between the middle electrical points was kept in $l = 2$ mm precisely.

RESULTS AND DISCUSSION

To understand the effects of reaction pressure on the properties of PPy films, several factors (thickness, UV-absorption, morphologies, and electrical conductivity) to evaluate the growth of the films under high pressure have been investigated and are discussed separately as follows.

Growth of PPy Films

The thickness of PPy films under different pressures were measured by AFM and are plotted in Fig. 1a. Under the same reaction pressure, the relationships between thickness and reaction time are approximately linearity. Therefore, the growth rate can be estimated by the relationships of film thickness and reaction time at that certain pressure. However, at the same time, higher pressure will increase the thickness of the film. The growth rate of PPy film on substrate under different pressure was calculated from Fig. 1a and was plotted in Fig. 1b using pressure as another axis. Our results clearly showed that the growth rate of PPy

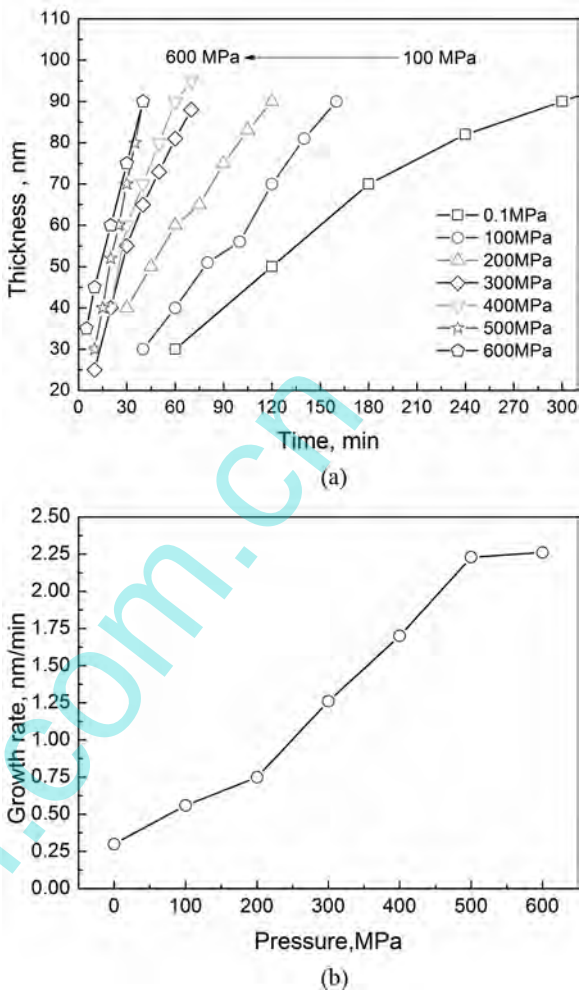

FIG. 1. (a) Thickness of PPy films prepared under different pressure; (b) The growth rate of PPy films under different pressure.

film was strongly related to the applied pressure during polymerization. As seen in Fig. 1b, the growth rate of PPy films was 0.31 nm/min under atmospheric pressure and increased rapidly to 2.23 nm/min under 500 MPa. Then, it slowly increased to 2.26 nm/min under 600 MPa. Note that the rate of growth under 500 MPa pressure was ~700% higher than that in atmospheric pressure.

It is well known that the growth of conducting polymer films on substrate in atmospheric pressure can be divided into three processes: the diffusion process, the adsorption process and the polymerization process. However, under high pressure, all processes were involved and affected the polymerization.

In the adsorption process, the adsorption of pyrrole monomer and oxidant plays an important role in forming the films. Firstly, the adsorption of pyrrole monomer on the substrate surface, which plays a key role as nucleation centers at the initial reaction stage. Secondly, the adsorption

of pyrrole monomer and oxidant greatly affects the local concentration in the polymerization process.

According to the theory of activated adsorption/desorption (TAAD) approach, the molecules in the activated state are in equilibrium with the reactants[22]. In the case of adsorption, the adsorbing molecules must pass through an activated state. Based on the classical TAAD approach, the surface coverage (θ) at the equilibrium as a function of the pressure and temperature was obtained recently by Panczyk and Rudzinski. It can be described by the following Langmuir isotherm equation[23]:

$$\theta(p,T) = \frac{Kpe^{\frac{\varepsilon}{kT}}}{1 + Kpe^{\frac{\varepsilon}{kT}}} \tag{1}$$

where K is the adsorption/desorption equilibrium constant and ε is the activation energy. To investigate the *in-situ* polymerization of PPy films, the Langmuir equation shown here is accepted as concentration of the reactants in our experiment is very low.

Obviously, when high pressure is applied to prepare PPy films, the surface coverage is enhanced compared to that in the ambient pressure case. Hence, the density of adsorbed pyrrole monomer on the substrate at the initial reaction stage is increased. This is obviously propitious to form the PPy film, i.e., increasing the growth rate of film.

In the polymerization process, the in-situ polymerization of PPy films occurred on the interfaces between aqueous phase and substrate/film. The rate of polymerization between the nucleation centers relates closely to the surface coverage. Some research results have also shown that hydrostatic pressure has a positive effect on the kinetics of polymerization[24,25]. It appears that the applied pressure during the reaction could alter the rate of polymerization differently.

In the case of polymerization in aqueous phase, the rate constant, namely k, is determined by Eq. (2):

$$\left(\frac{\partial lnK}{\partial P}\right)_T \cong -\frac{\Delta v^*}{RT} \tag{2}$$

where R is the gas constant, T is the absolute temperature, P is the applied pressure on the progress of reaction, and Δv^* is the activation volume. Generally speaking, the activation volume Δv^* is negative and almost constant. It was confirmed that high pressure applied in the reaction raises the rate constant of the polymerization in liquid. In addition, high pressure also increases the local concentration of the reactants in the reaction interfaces. This increase in the local concentration of reactants generally accelerates the reaction.

On the other hand, in the diffusion process, the compression of the reaction liquid caused by high pressure could raise the viscosity. The increase in viscosity slows the diffusion of reactants, expectantly. According to the Stokes–Einstein equation, the diffusion coefficient D_{di} of a spherical particle of radius r in a fluid of viscosity η at absolute temperature T is:

$$D_{di} = \frac{RT}{L \cdot 6\pi\eta \cdot \gamma} \tag{3}$$

where R is the gas constant and L is Avogadro's Number. It is clear that the high viscosity caused by high pressure reduces the diffusion of reactants in reaction liquid. The lack of reactants around the surface of substrate must restrain the growth of films.

As mentioned above, the higher reaction pressure has the advantage in the adsorption process and polymerization process but shows a negative effect in the diffusion process. In the case of lower pressure (<500 MPa), pressure has little effect on viscosity of the reaction liquid. The mutual effect of pressure on the reaction is that the increase in reaction rate by densification may be compensated by the decrease in the reaction rate with the increased viscosity of the liquid caused by the raised pressure[26].

The factor that the acceleration of growth of PPy film in the case of lower pressure may be interpreted by such an effect, that the increase in viscosity is insufficient to slow the reaction. In the case of higher pressure (>500 MPa), the viscosity of reaction liquid increased rapidly with the reaction pressure increasing. The high viscosity caused by high pressure reduces the diffusion of reactants. The rate of reaction was limited by the decreasing diffusion of reactants, which suggested that it was a diffusion controlling process.

Absorption Spectra of PPy Films

The UV-Vis absorption spectra for all as-prepared PPy films have been summarized in Fig. 2. A maximum

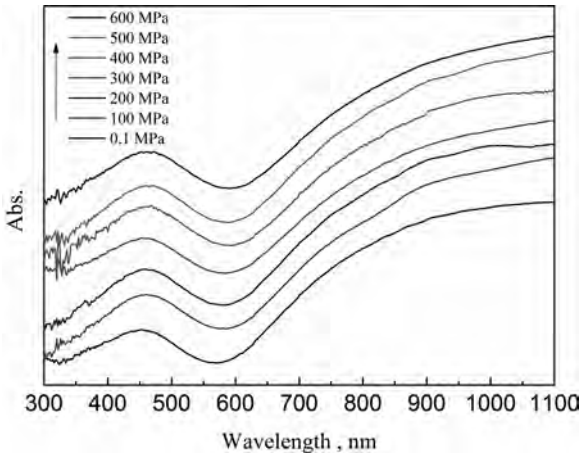

FIG. 2. UV–vis spectra of PPy films prepared at different applied pressure of 0.1, 100, 200, 300, 400, 500, and 600 MPa, respectively.

absorption band presented at around 450 nm and a high-intensity tail extending into the near IR region in the absorption spectra is also observed, the tailed peak was the typical characteristic of PPy and was attributed to the absorption of the antibonding and bonding bipolaron[27,28]. As shown in Fig. 2 and Table 1, there are relationships between pressure, UV–Vis absorption, I ratio and electrical conductivity of PPy films. For the film prepared at ambient pressure, the bipolaron absorption band appeared at 448 nm. However, this characteristic absorption band was sensitive to the applied pressure in the synthesis of the samples.

When the reaction pressure increased to 600 MPa, this absorption band shifted to 462 nm. Such a red-shift indicated that the conjugation length in the sample increased as the reaction pressure increased. Generally, the conjugation length was related to the conductivity of as-prepared polymer. Normally, the longer conjugation length the polymer has the larger electrical conductivity. The red-shift in UV-Vis absorption spectrum of our samples implied that the applied pressure in synthesis was helpful to improve the electrical conducting behavior.

Furthermore the absorption band of the bipolaron presented around 460 nm is related to the doping level and indicates the formation of polaron[28]. Based on the previous research that the extent of doping can roughly be estimated from the absorption spectra of the PPy film, the *I* (intensity ratio) of max absorbance band around 460 nm and minimum absorbance band around 600 nm can be used to indicate the doping level of PPy film. In Table 1, the I (intensity ratio) first increases as the pressure of the reaction increases from ambient pressure to 400 MPa and then decreases slowly as the pressure continue to increase to 600 MPa. The similar variation in UV-vis absorption spectrum was also observed by Mikat et al.[29]

TABLE 1
Relationship between pressure, UV–Vis absorption, I (intensity ratio) and electrical conductivity of PPy films

Pressure (MPa)	Anti-bonding bipolaron band	I*	Conductivity (S/cm)
0.1	448 nm	1.162	27.9
100	452 nm	1.164	29.7
200	456 nm	1.168	35.4
300	458 nm	1.176	38.6
400	460 nm	1.190	42.3
500	462 nm	1.189	41.7
600	462 nm	1.181	40.3

*I (intensity ratio) is the maximum absorption band of the anti-bonding bipolaron presented around 460 nm divided by minimum absorbance band around 600 nm.

They found that the intensity of absorption around 460 nm became weaker when high pressure was applied for the PPy film prepared at atmosphere. The decrease of intensity values for the absorption band at a high pressure indicates a transition from a bipolaron dominated structure to a more polaron structure according to their research. It is well known that the doping level of bipolaron structure is higher than polaron structure. The changed doping level implied that, the applied high pressure affects the types of carriers, and restrains the improvement of the electrical conducting behavior.

Furthermore, the FT-IR spectra of PPy films synthesized under different pressures were measured (Fig. 3). The strong absorption bands near 990 and 786 cm^{-1} are characteristic peaks of quartz glass in the spectrum. Some of the absorption peaks belonged to PPy films fall in the same region as do the quartz glass absorptions, thereby causing overlap. There are four clear absorption peaks of PPy films that can be observed, and these peaks' positions are listed in Table 2. The band at 1545 cm^{-1} for the sample prepared at ambient pressure is assigned to C-C stretching vibrations in the pyrrole ring, which will red-shift to the lower wavenumbers (1541 cm^{-1}) when the applied pressure goes up to 600 MPa. This is connected with the influence of the doping on the skeletal vibrations, involving the delocalized π-electrons.

The band of the C-N stretching vibration in the ring, appeared at 1458 cm^{-1} for the sample prepared under ambient pressure, is shifted to 1450 cm^{-1} for the sample prepared under high pressure. The broad band from 1400 to 1250 cm^{-1} is attributed to C-H or C-N in-plane deformation modes, and has a maximum at 1300 cm^{-1}. There is no obvious change for the position of this absorption band. In the region of the C-H and N-H in-plane deformation from 1250 to 1000 cm^{-1}, maximum peaks at 1168 cm^{-1}

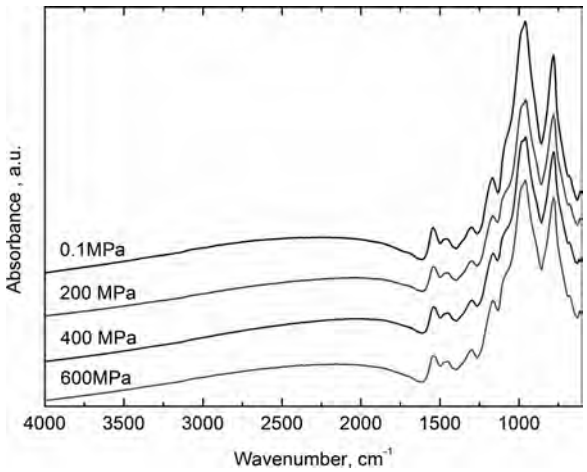

FIG. 3. The FT-IR spectra of the PPy films prepared at different applied pressure respectively.

TABLE 2
FT-IR parameters of PPy films prepared under different applied pressure

Pressure (MPa)	Ring stretching mode		C–H or C–N in-plane deformation	C–H and N–H in-plane deformation vibrations	I(symmetric)/ I(antisymmetric)
	Antisymmetric	Symmetric			
0.1	1545	1458	1300	1169	0.9053
200	1543	1456	1298	1165	0.9388
400	1541	1452	1298	1163	0.9440
600	1543	1450	1298	1165	0.9407

and 1163 cm^{-1} are for the sample prepared under ambient pressure and under high pressure, respectively.

The group at 1480/1540 cm^{-1}, assigned to the symmetric and anti-symmetric ring stretching mode, respectively, is used as an indicator for the conjugation. The higher the ratio is, the better the conjugation is[30]. According to the analysis by Tian and Zerbi, the ratio of the integrated absorption intensities of the 1560 and 1480 cm^{-1} band I1560/I1480 is inversely proportional to the extent of delocalization. Thus, polymers with high concentrations of defect sites (short conjugation lengths) showed high values of I1560/I1480, whereas polymers with low concentrations of defect sites (long conjugation lengths) showed low values of I1560/I1480[31,32]. Therefore, the ratio of the intensities I1460/I1540 determines the extent of the conjugation in this paper, the calculated results were listed in Table 2. The ratio is represented in the ascending order from 0.1 to 400 MPa, but there is only a tiny change from 400 to 600 MPa.

From the preceding results, it is very difficult to give a clear linearity between the applied pressure and the conjugation. Generally speaking, the high pressure enhances the conjugation along the polymer backbone. But pressure effect on polymerization is more complicated. Mikat and his coauthors have already mentioned that the symmetric ring stretching band at 1480 cm^{-1} becomes broader and eventually merges into the underground, while the anti-symmetric ring stretching band at 1540 cm^{-1} remains almost constant in intensity and position at the high measure pressure (>1 GPa).

Pressure usually induces the sharpening of vibrational bands due to the elimination of conformational defects. The broadening of the band at 1480 cm^{-1} would imply that a strong pressure could induce the distortion of the symmetric vibration whereas the anti-symmetric vibration would be unaffected[29]. Therefore, it is clear that the usual method for the determination of the conjugation is not applicable for the PPy spectra under very high pressure. Maybe the effect of high reaction pressure is similar to the high measured pressure. But under high reaction pressure (100–600 MPa), a better conjugation is expected simultaneously. The red-shift in the FT-IR and UV-Vis spectra also supported this assumption.

Morphology of the Films

The surface morphologies of the PPy films prepared at different pressure and reaction times have been studied by SEM. Typical surface images are presented in Fig. 4. As shown in Fig. 4a, the film polymerized at ambient pressure usually gave a typical granular morphology. However, with the increased polymerization times (Figs. 4b and 4c), many wrinkles started to appear on the surface of PPy film. This morphology of PPy films was ubiquitously observed in these samples, prepared through electrochemical polymerization on many different material surfaces. Under high pressure although there was no obvious change in granular morphology of PPy films, the surface of PPy film became smoother. In Figs. 4e and 4f, the wrinkles also appeared in the surface of PPy film prepared under high pressure. But the quantity and the height of wrinkles decreased under high pressure when compared to the ambient pressure case.

It is well known that the wrinkles greatly affect the mechanical properties, optical transmittance and conductivity of the films. In some previous reports, the mechanism of the formation of wrinkles is complicated[33–36]. Also the wrinkles were suddenly found to appear during film thickness increasing. The morphology of wrinkles could be controlled by many factors such as nature of the substrates, nature and size of the dopant ions, solvent, and concentrations of pyrrole and dopant[34,35]. Our experiments suggest that the pressure was identified as the decisive factor to control the morphology of wrinkles. The high pressure may depress the wrinkling effectively and make the films more smooth, which could effectively improve the properties of the PPy films. However, the mechanism for pressure how to affect the wrinkles growth is still not well established in our study.

For further study on the details of granular morphology, AFM has been employed to study the surface morphology of the as-prepared films. Figure 5 shows the typical AFM images of PPy films, which have similar thickness under different pressure: 0.1 MPa (Figs. 5a and 5c) and 600 MPa (Figs. 5b and 5d), respectively. The size of the image (a) and (b) are 10 μm × 10 μm and

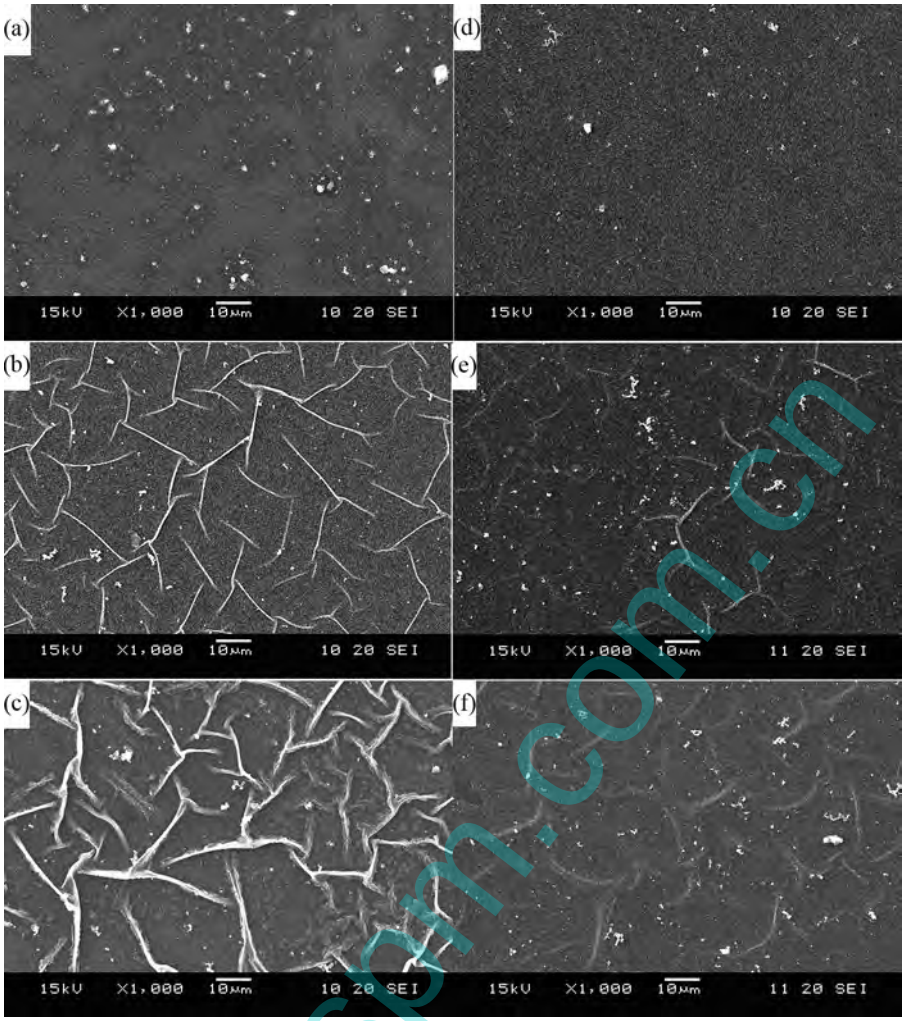

FIG. 4. SEM of PPy films prepared in different reaction condition: (a) 0.1 MPa, 2 hour; (b) 0.1 MPa, 4 hour; (c) 0.1 MPa, 6 hour; (d) 600 MPa, 10 min; (e) 600 MPa, 20 min; (f) 600 MPa, 30 min.

images 5c and 5d are 3000 nm × 3000 nm. The AFM images reveal a surface topography of typical granular patterns and the spheres with a diameter of ~90 nm. Table 3 summarizes all AFM parameters of PPy films under different pressure. The AFM images of PPy films prepared under high pressure indicate a decreasing surface roughness, a smaller particle diameter and a lower peak height. The results of AFM experiment suggest that pressure has a weak effect on the formation of granular morphology, but has a big effect on the close packing of granular morphology.

Our previous studies showed that the morphology of PANI films as well as the properties changed a lot under high pressure. However, since the growth mechanism of PPy films is different from that of PANI film, the properties of PPy films prepared under high pressure have smaller changes comparing to that of PANI films in our previous study.

Electrical Conductivity of the Films

By measuring the resistance R of PPy films, the value of conductivity can be determined according to the following equation:

$$\sigma = \frac{l}{RS} \tag{4}$$

$$S = W \times H \tag{5}$$

where l is the distance between the middle electrical points, W the width (6 mm), and H the thickness, respectively. The conductivity of PPy films was plotted in Fig. 6a. According to the experimental results, the reaction-time dependence of conductivity under high pressure is the same as that under atmospheric pressure. Initially, the conductivity increased with the reaction time increasing. When the conductivity reached a certain number, it no longer increased

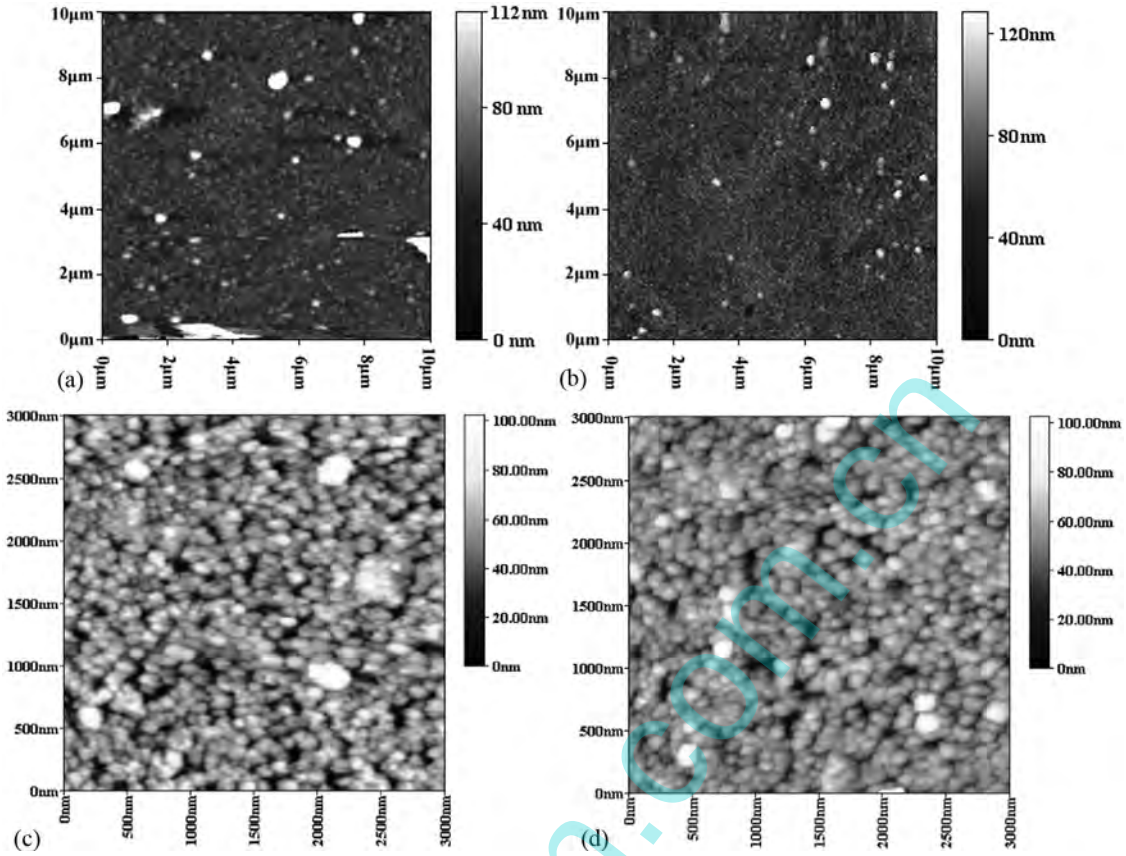

FIG. 5. AFM images of the PPy films prepared under different pressure: (a)(b) 0.1 MPa; (c)(d) 600 MPa.

with the increasing reaction time. In this stage, some wrinkles appeared on its surface and the thickness of films is hard to measure by AFM. The surface resistance of PPy films was also influenced by wrinkles. Therefore the measurement of conductivity became inaccurately. It was considered that the maximum conductivity in the beginning of second step was the optimum conductivity under different pressure.

It is obvious that there is a strong relationship between conductivity, reaction time and applied pressure. From Fig. 6b, the optimum conditions are determined: the applied pressure was 400 MPa and reaction time was 40 to 50 min. As shown in Table 1, the maximum conductivity of PPy films was strongly related to the applied pressure in reaction. The maximum conductivity of PPy films was 27.99 S/cm under atmospheric pressure and increased to 42.31 S/cm under 400 MPa. It is noteworthy that the conductivity decreased slowly when the reaction pressure increased to 600 MPa. Electrical conductivity of any inherently conductive polymer depends on its molecular structure: the more closely packed and more oriented molecule chains with long conjugation length, the better conductivity is achieved. The results of UV-Vis, FT-IR and AFM experiment suggest that the pressure affects effectively on the conjugation length and close packing. It is reasonable to consider that the high reaction pressure should be a positive factor to enhance the electrical conductivity of PPy films.

However, our experimental results imply that the high pressure applied in the reaction strongly raises the growth rate of films and changes the type of carriers. Generally speaking, the higher rate of growth could cause more defects in film. This factor obviously reduces the conductivity of films prepared under high pressure. This phenomenon is similar to that of the changes for conductivity of PANI films prepared under high pressure in our previous

TABLE 3
AFM parameters of PPy films prepared under different pressure

Pressure (MPa)	Surface roughness RMS (nm)	Surface particle size analysis	
		Average size cluster circular (φ) nm	Average grains height (nm)
0.1	10.6	86.8	64.9
600	7.7	82.3	60.5

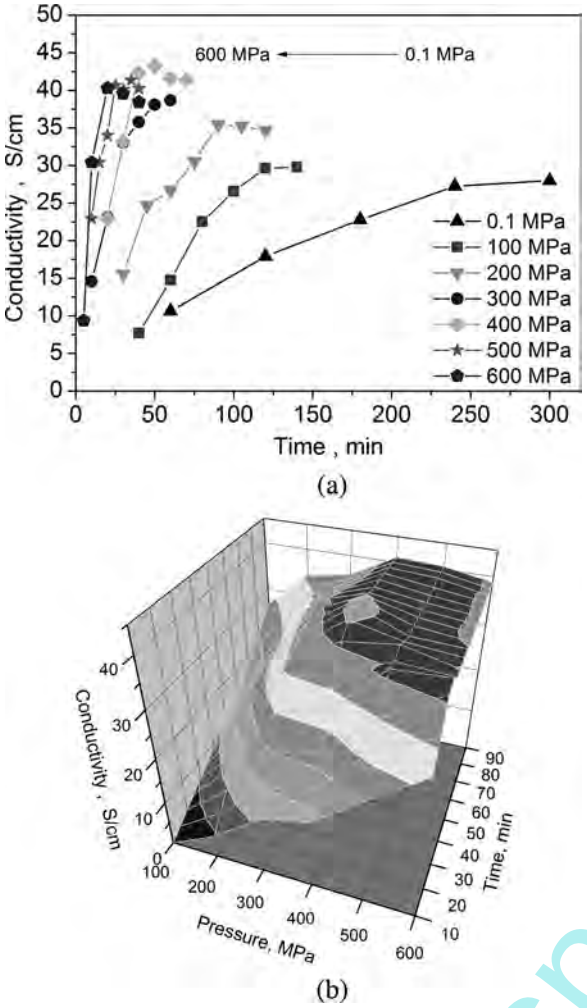

FIG. 6. The relationship between conductivity, reaction time and applied pressure: (a) The conductivity of PPy films at different applied pressure of 0.1, 100, 200, 300, 400, 500, and 600 MPa, respectively. (b) The three-dimensional graph constructed according to the data by computer.

studies[18–20]. Although the conductivity of PPy films prepared under high pressure could increase by 50%, PANI films prepared at the same condition didn't show such promising results. The optimum reaction pressure of PPy film is around 400 MPa.

CONCLUSIONS

We have systematically studied the influence of the reaction pressure in *in-situ* polymerization on the properties of polypyrrole films. It is found that the growth rate of PPy film was strongly dependant on the applied pressure in polymerization. In high reaction pressure, the rate of growth has ~700% increasing comparing that in atmospheric pressure. The surface morphology of PPy films polymerized under high pressure becomes much smoother. When the applied reaction pressure is 400 MPa and the optimized reaction time is 40 min, the as-prepared PPy films show a better conductivity as high as 42.31 S/cm. The enhancement of conjugation length and close packing are the reasons for a better electrical property of PPy films when the films were prepared under high reaction pressure. These results may provide a good reference for in-situ polymerization of pyrrole and its derivatives under high reaction pressure.

FUNDING

This work was supported by National Natural Science Foundation of China (NSFC 10774076), Natural Science Fund for Colleges and Universities in Jiangsu Province (09KJB140003 and 11KJB480003), Jiangsu Planned Projects for Postdoctoral Research Funds (1301036C) and Open Project M25021 of National Laboratory of Solid State Microstructures in Nanjing University.

REFERENCES

1. MacDiarmid, A.G. "Synthetic metals": A novel role for organic polymers (Nobel lecture). Angew. Chem. Int. Ed. **2001**, *40*, 2581–2590.
2. Simonet, J.; Rault-Berthelot, J. Electrochemistry: A technique to form, to modify and to characterize organic conducting polymers. Prog. Solid State Chem. **1991**, *21*, 1–48.
3. Ishiguro, T.; Kaneko, H.; Nogami, Y.; Ishimoto, H.; Nishiyama, H.; Tsukamoto, J.; Takahashi, A.; Yamaura, M.; Hagiwara, T.; Sato, K. Logarithmic temperature dependence of resistivity in heavily doped conducting polymers at low temperature. Phys. Rev. Lett. **1992**, *69*, 660–663.
4. Sato, K.; Yamaura, M.; Hagiwara, T.; Murata, K.; Tokumoto, M. Study on the electrical conduction mechanism of polypyrrole films. Synth. Met. **1991**, *40*, 35–48.
5. Yamaura, M.; Hagiwara, T.; Iwata, K. Enhancement of electrical conductivity of polypyrrole film by stretching: Counter ion effect. Synth. Met. **1988**, *26*, 209–224.
6. Barnoss, S.; Shanak, H.; Bof Bufon, C.C.; Heinzel, T. Piezoresistance in chemically synthesized polypyrrole thin films. Sens. Actu. A **2009**, *154*, 79–84.
7. Otero, T.F.; Martinez, J.G.; Fuchiwaki, M.; Valero, L. Structural electrochemistry from freestanding polypyrrole films: Full hydrogen inhibition from aqueous solutions. Adv. Funct. Mater. **2014**, *24*, 1265–1274.
8. Song, X.; Gong, H.; Yin, S.; Cheng, L.; Wang, C.; Li, Z.; Li, Y.; Wang, X.; Liu, G.; Liu, Z. Ultra-small iron oxide doped polypyrrole nanoparticles for in vivo multimodal imaging guided photothermal therapy. Adv. Funct. Mater. **2014**, *24*, 1194–1201.
9. Zhang, G.; Yang, F. Electrocatalytic reduction of dioxygen at glassy carbon electrodes modified with polypyrrole/anthraquinonedisulphonate composite film in various pH solutions. Electrochim. Acta **2007**, *52*, 6595–6603.
10. Zhang, G.; Yang, F.; Gao, M.; Liu, L. Electrocatalytic behavior of the bare and the anthraquinonedisulfonate/polypyrrole composite film modified graphite cathodes in the electro-Fenton system. J. Phys. Chem. C **2008**, *112*, 8957–8962.
11. Das, T.K.; Prusty, S. Review on conducting polymers and their applications. Polym.-Plast. Technol. Eng. **2012**, *51*, 1487–1500.
12. Li, X.-G.; Li, A.; Huang, M.-R.; Liao, Y.; Lu, Y.-G. Efficient and scalable synthesis of pure polypyrrole nanoparticles applicable for advanced nanocomposites and carbon nanoparticles. J. Phys. Chem. C **2010**, *114*, 19244–19255.
13. Li, X.-G.; Hou, Z.-Z.; Huang, M.-R.; Moloney, M.G. Efficient synthesis of intrinsically conducting polypyrrole nanoparticles containing

hydroxy sulfoaniline as key self-stabilized units. J. Phys. Chem. C **2009**, *113*, 21586–21595.
14. Yoon, C.O.; Reghu, M.; Moses, D.; Heeger, A.J. Transport near the metal-insulator transition: polypyrrole doped with PF6. Phys. Rev. B: Condens. Matter **1994**, *49*, 10851–10863.
15. Kohlman, R.S.; Joo, J.; Wang, Y.Z.; Pouget, J.P.; Kaneko, H.; Ishiguro, T.; Epstein, A.J. Drude metallic response of polypyrrole. Phys. Rev. Lett. **1995**, *74*, 773–776.
16. Yamamura, M.; Hagiwara, T.; Iwata, K. Synth. Met. **1988**, *26*, 209.
17. Lee, K.; Menon, R.; Yoon, C.O.; Heeger, A.J. Reflectance of conducting polypyrrole: Observation of the metal-insulator transition driven by disorder. Phys. Rev. B: Condens. Matt. **1995**, *52*, 4779–4787.
18. Sixou, B.; Mermilliod, N.; Travers, J.P. Aging effects on the transport properties in conducting polymer polypyrrole. Phys. Rev. B: Condens. Matter **1996**, *53*, 4509–4521.
19. Gu, D.W.; Li, J.S.; Liu, J.L.; Cai, Y.M.; Shen, L.J. Polyaniline thin films in situ polymerized under very high pressure. Synth. Met. **2005**, *150*, 175–179.
20. Li, J.S.; Shen, L.J.; Gu, D.W.; Yuan, P.F.; Cui, X.B.; Yang, N.R. Optimum conditions for the preparation of polyaniline films under very high pressure. React. Funct. Polym. **2006**, *66*, 1319–1326.
21. Shen, L.J.; Gu, D.W.; Li, J.S.; Zhou, H.Y.; Xiao, W.R.; Yang, N.R. The growth of PANI films at 450 MPa. Synth. Met. **2005**, *155*, 110–115.
22. Clark, C.A. *The Theory of Adsorption and Catalysis*, Academic Press: New York, 1970.
23. Panczyk, T.; Rudzinski, W. A statistical rate theory approach to kinetics of dissociative gas adsorption on solids. J. Phys. Chem. B **2004**, *108*, 2898–2909.
24. Wasylyshyn, D.A.; Johari, G.P. Molecular dynamics and reaction kinetics during the network structure formation of a diepoxide and diamine mixture under high pressures using dielectric measurements. J. Chem. Soc. Farad. Trans. **1997**, *93*, 4025–4032.
25. Wang, J.; Johari, G.P. The gradual transition from mass-controlled to diffusion-controlled kinetics during melt polymerization. J. Chem. Phys. **2002**, *117*, 9897–9902.
26. Wasylyshyn, D.A.; Johari, G.P. Dielectric effects of step-increased pressure on the mass- and diffusion-controlled linear chain and network macromolecules growth. Chem. Phys. **1998**, *237*, 345–358.
27. Furukawa, Y.; Tazawa, S.; Fujii, Y.; Harada, I. Raman spectra of polypyrrole and its 2,5–13C-substituted and C-deuterated analogues in doped and undoped states. Synth. Met. **1988**, *24*, 329–341.
28. Hu, Y.; Yang, R.; Evans, D.F.; Weaver, J.H. Direct measurements of bipolaron-band development in doped polypyrrole with inverse photoemission. Phys. Rev. B **1991**, *44*, 13660–13665.
29. Mikat, J.; Orgzall, I.; Hochheimer, H.D. Optical absorption and vibrational spectroscopy of conducting polypyrrole under pressure. Synth. Met. **2001**, *116*, 167–170.
30. Lei, J.; Cai, Z.; Martin, C.R. Effect of reagent concentrations used to synthesize polypyrrole on the chemical characteristics and optical and electronic properties of the resulting polymer. Synth. Met. **1992**, *46*, 53–69.
31. Carrasco, P.M.; Grande, H.J.; Cortazar, M.; Alberdi, J.M.; Areizaga, J.; Pomposo, J.A. Structure–conductivity relationships in chemical polypyrroles of low, medium and high conductivity. Synth. Met. **2006**, *156*, 420–425.
32. Tian, B.; Zerbi, G. Lattice dynamics and vibrational spectra of pristine and doped polypyrrole: Effective conjugation coordinate. J. Chem. Phys. **1990**, *92*, 3892–3898.
33. Shapiro, J.S.; Smith, W.T.; MacRae, C. Wrinkle morphology of polypyrrole films grown in thin-layer cells. Synth. Met. **1995**, *69*, 505–506.
34. Shapiro, J.S.; Smith, W.T. A morphological study of polypyrrole films grown on indium-tin oxide conductive glass. Polymer **1997**, *38*, 5505–5514.
35. Miles, M.J.; Smith, W.T.; Shapiro, J.S. Morphological investigation by atomic force microscopy and light microscopy of electropolymerised polypyrrole films. Polymer **2000**, *41*, 3349–3356.
36. Wu, J.-S.; Gu, D.-W.; Huang, D.; Shen, L.-J. Chemical in situ polymerization of polypyrrole nanoparticles on the hydrophilic/hydrophobic surface of SiO_2 substrates. Synth. React. Inorg. Met-Org. Nano-Met. Chem. **2012**, *42*, 1064–1070.